

# PCCP

Accepted Manuscript



This is an *Accepted Manuscript*, which has been through the Royal Society of Chemistry peer review process and has been accepted for publication.

*Accepted Manuscripts* are published online shortly after acceptance, before technical editing, formatting and proof reading. Using this free service, authors can make their results available to the community, in citable form, before we publish the edited article. We will replace this *Accepted Manuscript* with the edited and formatted *Advance Article* as soon as it is available.

You can find more information about *Accepted Manuscripts* in the [Information for Authors](#).

Please note that technical editing may introduce minor changes to the text and/or graphics, which may alter content. The journal's standard [Terms & Conditions](#) and the [Ethical guidelines](#) still apply. In no event shall the Royal Society of Chemistry be held responsible for any errors or omissions in this *Accepted Manuscript* or any consequences arising from the use of any information it contains.

**Gramicidin A disassembles large  
conductive clusters of its lysine-substituted derivatives in lipid membranes**

Yuri N. Antonenko<sup>1</sup>, Grigory Gluhov<sup>2</sup>, Alexander Firsov<sup>1</sup>, Irina Pogozheva<sup>3</sup>, Sergey I. Kovalchuk<sup>4</sup>, Eugenia Pechnikova<sup>5</sup>, Elena A. Kotova<sup>1</sup>, Olga Sokolova<sup>2</sup>

<sup>1</sup>*Belozersky Institute of Physico-Chemical Biology, Lomonosov Moscow State University, Moscow, Russia*

<sup>2</sup>*Department of Bioengineering, Faculty of Biology, Lomonosov Moscow State University, Moscow, Russia*

<sup>3</sup>*Department of Medicinal Chemistry, University of Michigan, Ann Arbor, MI, USA*

<sup>4</sup>*M.M.Shemyakin and Y.A.Ovchinnikov Institute of Bioorganic Chemistry, Russian Academy of Sciences, Moscow, Russia*

<sup>5</sup>*A.V.Shoubnikov Institute of Crystallography, Russian Academy of Sciences, Moscow, Russia*

**Address correspondence to:** Yuri Antonenko, Belozersky Institute of Physico-Chemical Biology, Lomonosov Moscow State University, Moscow 119991, Russia.  
Fax: +(7-495)-939-31-81, E-mail: antonen@genebee.msu.ru

**Keywords:** peptide, liposome, leakage, pore, channel, permeability, gramicidin A, cryo-electron microscopy

RUNNING TITLE: Cation- $\pi$  interactions in conductive gramicidin clusters

---

**Abbreviations:** gA, gramicidin A; [Lys3gA], gA with lysine in the position 3 instead of alanine; EggPC, egg yolk phosphatidylcholine; SRB, sulforhodamine B; CF, carboxyfluorescein; BLM, bilayer lipid membrane; FCS, fluorescence correlation spectroscopy; TEM, transmission cryo-electron microscopy

## ABSTRACT

N-terminally substituted lysine derivatives of gramicidin A (gA), [Lys1]gA and [Lys3]gA, but not glutamate- or aspartate-substituted peptides have been previously shown to cause leakage of carboxyfluorescein from liposomes. Here, the leakage induction was also observed for [Arg1]gA and [Arg3]gA, while [His1]gA and [His3]gA were inactive at neutral pH. The Lys3-containing analogue with all tryptophans replaced by isoleucines did not induce liposome leakage, similar to gA, which favors the presence of both tryptophans and N-terminal cationic residues to be critical for pore formation. Remarkably, the addition of gA blocked the leakage induced by [Lys3]gA. By examining with fluorescence correlation spectroscopy the peptide-induced leakage of fluorescent markers from liposomes, we estimated the diameter of pores responsible for the leakage to be about 1.6 nm. Transmission electron cryo-microscopy imaging of liposomes with [Lys3]gA showed that the liposomal membranes contained high electron density particles with a size of about 40 Å, suggesting formation of peptide clusters. No such clusterization was observed in liposomes incorporating gA or a mixture of gA with [Lys3]gA. Three-dimensional reconstruction of the clusters was compatible with their pentameric arrangement. Based on experimental data and computational modeling, we suggest that the large pore formed by [Lys3]gA represents a barrel-stave oligomeric cluster formed by antiparallel double-stranded helical dimers (DH). In a tentative model, the pentamer of dimers may be stabilized by aromatic Trp-Trp and cation- $\pi$  Trp-Lys interactions between the neighboring DHs. The inhibiting effect of gA on the [Lys3]gA-induced leakage can be attributed to breaking cation- $\pi$  interactions, which prevents peptide clusterization and pore formation.

## 1. Introduction

The potent antibiotic gramicidin A (gA) produced by *Bacillus brevis* was discovered in the 30s of the 20th century,<sup>1</sup> but the high hemolytic activity of this 15-mer linear peptide and toxicity toward eukaryotic cells<sup>2,3</sup> hindered its therapeutic application. In medicinal practice gA is currently used only as topical contraceptive and antimicrobial.<sup>4</sup> This hydrophobic peptide has become a classical object of biophysical studies due to its ability to form ion-conducting channels in lipid membranes with high selectivity to monovalent cations and well-defined single-channel parameters, i.e. unitary conductance and lifetime.<sup>5-7</sup> Electrophysiological experiments have revealed strong sensitivity of gA single-channel properties to sequence substitutions, especially at the N-terminus,<sup>8-14</sup> thus supporting the head-to-head single-stranded helical dimer (HD) structure of the gA channel.<sup>15-20</sup> These findings stimulated research efforts aimed at design of gA derivatives having reduced toxicity toward eukaryotic cells, but retaining high antimicrobial activity.<sup>21-23</sup> In particular, a lactam-bridged gA analogue was reported to exhibit a typically high antibiotic potency of gA in combination with low hemolytic activity and suppressed toxicity toward mammalian cells.<sup>23</sup> Another step forward was associated with design of the [Glu1]gA analogue with decreased cytotoxicity, which may have therapeutic potential by protecting brain from perfusion- or ischemia-induced neuronal cell death.<sup>24</sup> Besides, possible applications as anticancer drugs were found not only for gA and its derivatives,<sup>25</sup> but also for combinations of gA with curcumin<sup>3</sup> or the pH (Low) Insertion Peptide.<sup>26</sup>

According to our previous works,<sup>27,28</sup> Lys-substituted gA analogues induced not only potassium conductance, typical of gA channels, but also pores of much larger conductance that were unselective with respect to monovalent cation conductivity and permeable to such compounds as carboxyfluorescein (CF) and sulforhodamine B (SRB). Interestingly, induction of unselective conductance by the Lys-substituted peptides essentially depended on the lysine position in the gA sequence, being maximal for [Lys3]gA among Lys-substitutions in the positions 1, 3, and 5.<sup>28</sup> The gA analogues with C-terminal polycationic extensions also appeared to be able to form unselective pores in lipid membranes.<sup>29,30</sup> The mechanism of formation of pores permeable to fluorescent markers remains unclear, albeit data of fluorescent correlation spectroscopy (FCS) have proved the retention of membrane integrity in the presence of the gA analogues.<sup>28</sup>

Gramicidin is known to adopt different conformations in diverse solvents and membranes, including head-to-head right-handed single-stranded helical dimers (HD) and

parallel and antiparallel (left- and right-handed) double-stranded helical dimers (DH).<sup>31,32</sup> At conformational equilibrium of gA, the relative contributions of different forms depend on the nature of the organic solvent<sup>32</sup> or on the lipid bilayer composition.<sup>33</sup> According to CD spectra, [Lys3]gA in liposomal membranes is predominantly in the form of antiparallel DH at pH 7, while alkalization of the medium resulted in an increase in the contribution of the head-to-head HD structure of the gA channel form.<sup>27</sup> Based on these data, the unselective channels were tentatively attributed to barrel-stave oligomeric arrangement of double helices.<sup>30</sup> Of note, at high concentrations gA can yield densely packed quasi-regular structure, presumably formed of peptide oligomers.<sup>34</sup> Also of relevance is the tendency of polycationic and polyanionic analogues to clusterization in lipid membranes in the presence of polyelectrolytes in low ionic strength bathing solutions.<sup>35,36</sup>

Here, we studied the structure of unselective channels by transmission cryo-electron microscopy (TEM). Consistent with the above-mentioned model of the unselective pore,<sup>30</sup> the TEM images of [Lys3]gA in liposomes were approximated by circular pentameric arrangement of antiparallel right-handed DH dimers (comprising 10 peptide monomers) stabilized by aromatic interaction of multiple tryptophan residues and cation- $\pi$  interactions between tryptophans and lysines of neighboring dimers. The addition of unaltered gA was found here to inhibit the unselective pore formation by [Lys3]gA, which could be due to interaction between tryptophans of gA and [Lys3]gA leading to disturbance of the circular barrel-stave arrangement of [Lys3]gA double helices and formation of linear aggregates of gA and [Lys3]gA without an aqueous channel lumen.

## 2. Experimental details

### 2.1 Peptides and other chemicals

All reagents and solvents were obtained from commercial sources and used without additional purification. Egg yolk phosphatidylcholine (EggPC) and total lipid of *Escherichia coli* were from Avanti Polar Lipids (Alabaster, AL), soybean phosphatidylcholine (Type II-S) and bovine heart cardiolipin were from Sigma-Aldrich (Steinheim, Germany). Gramicidin A (gA; HCO-L-Val<sup>1</sup>-Gly<sup>2</sup>-L-Ala<sup>3</sup>-D-Leu<sup>4</sup>-L-Ala<sup>5</sup>-D-Val<sup>6</sup>-L-Val<sup>7</sup>-D-Val<sup>8</sup>-L-Trp<sup>9</sup>-D-Leu<sup>10</sup>-L-Trp<sup>11</sup>-D-Leu<sup>12</sup>-L-Trp<sup>13</sup>-D-Leu<sup>14</sup>-D-Trp<sup>15</sup>-NH(CH<sub>2</sub>)<sub>2</sub>OH) was from Fluka. Analogs of gA, [Glu1]gA, [Glu3]gA, [Asp1]gA, [Lys1]gA, [Lys3]gA, [Arg1]gA, [Arg3]gA, [His1]gA, [His3]gA, and Trp-free cationic gA analogue [Lys3Ile9Ile11Ile13Ile15]gA, were prepared by

standard solid-phase  $N\alpha$ -Fmoc methodology on 2-chlorotriyl chloride polystyrene resin using the diisopropylcarbodiimide/1-hydroxybenzotriazole coupling system. N-terminal formylation of peptides was conducted in the presence of N-ethyl-diisopropylamine using 2-nitrophenyl formate.<sup>27,37</sup> The peptides were cleaved from the polymer and deprotected with trifluoroacetic acid-1,2-ethanedithiol-triisopropylsilane-water (95:2:2:1) for 2.5 h. Peptides were purified with RP-HPLC to the rate >95 %. The identity of peptides was confirmed by MALDI-TOF MS.

## 2.2 Liposome preparation

Liposomes were prepared by evaporation under a stream of nitrogen of a 2 % solution of a lipid in chloroform followed by hydration with aqueous buffer solution containing appropriate fluorescent marker. The mixture was vortexed, passed through a cycle of freezing and thawing, and extruded through 0.1- $\mu$ m pore size Nucleopore polycarbonate membranes using an Avanti Mini-Extruder.

## 2.3 Leakage assay using fluorescence de-quenching method

Liposomes were prepared from EggPC in presence of CF (100 mM). The extra-liposomal CF was removed by passage of the liposome suspension through a Sephadex G-50 coarse column using Tris/MES eluting buffer (100 mM KCl, 10 mM Tris, 10 mM MES), pH 7.0. To measure the rate of CF efflux in the presence of gA analogues, liposomes were diluted in Tris/MES buffer, pH 7.0 and the fluorescence at 520 nm (excitation at 490 nm) was monitored with a Panorama Fluorat 02 spectrofluorimeter (Lumex, Russia). At the end of each recording, 0.1% Triton-X100 was added to complete the efflux process.

## 2.4 Leakage assay using fluorescence correlation spectroscopy (FCS)

Liposomes were prepared from soybean phosphatidylcholine (PC, 4 mg in a sample) and bovine heart cardiolipin (1 mg in a sample) dispersed in 0.5 ml of Tris/MES buffer (pH 7.0) in the presence of fluorescent markers: 1 mM SRB, 3 mg/ml rhodamine-labeled 3-kDa dextran or 10 mg/ml rhodamine-labeled 10-kDa dextran. The unbound marker was removed by passage of the liposome suspension through a Sephadex G-50 coarse column (for SRB) or through a Sephadex G-150 coarse column using Tris/MES eluting buffer (pH 7.0). FCS measurements were carried out with a home-made FCS setup,<sup>38-40</sup> including an Olympus IMT-2 inverted microscope with a 40x, NA 1.2 water immersion objective (Carl Zeiss, Jena, Germany). A

Nd:YAG solid state laser was used for excitation of SRB at 532 nm. The fluorescence that passed through an appropriate dichroic beam splitter and a long-pass filter was imaged onto a 50- $\mu\text{m}$  core fiber coupled to an avalanche photodiode (PerkinElmer Optoelectronics, Fremont, CA). The signal from an output was correlated by a correlator card (Correlator.com, Bridgewater, NJ). The data acquisition time was 120 s, and 3 to 5 curves were averaged.

Experimental curves were fitted by the correlation function for three-dimensional diffusion:<sup>41,42</sup>

$$G(\tau) = 1 + \frac{1}{N} \left( \frac{1}{1 + \frac{\tau}{\tau_D}} \right) \left( \frac{1}{\sqrt{1 + \frac{r_0^2 \tau}{z_0^2 \tau_D}}} \right)$$

with  $\tau_D$  being the characteristic diffusion time during which a molecule resides in the cylindrical observation volume of radius  $r_0$  and length  $z_0$ , given by  $\tau_D = r_0^2/4D$ , where  $D$  is the diffusion coefficient,  $N$  is the mean number of molecules in the confocal volume.

## 2.5 Transmission electron cryo-microscopy (TEM) and image processing

Liposomes were prepared from 10 mg EggPC dissolved in 100  $\mu\text{l}$  of ethanol containing 10  $\mu\text{g}$  gA, 10  $\mu\text{g}$  [Lys3]gA, or both peptides. The suspension of liposomes in Tris/MES buffer (pH 7.0) with and without gA and [Lys3]gA was quickly frozen in liquid ethane using Vitrobot Mark IV (FEI, Netherlands). Cryo-micrographs were taken with FEI Tecnai G2 Spirit TEM, 120 kV working voltage at 26,000x magnification, under low-dose conditions (the dose was less than 20  $\text{e}/\text{\AA}^2$ ), using defocii in the range of 2.5-3.5  $\mu\text{m}$ . Images were captured with a CCD camera Eagle (FEI). The pixel size on the micrograph was 5.3  $\text{\AA}$ . Parts of liposome images (90x90 pixels) were cut from the micrographs using the program BOXER,<sup>43</sup> band-pass filtered, aligned first against the rotational average, then against a total sum of all previously aligned images, as implemented in the program IMAGIC.<sup>44</sup> Stable classes were obtained after four iterations of alignment. To measure the thickness of liposomal membranes, all images within a class were summarized and the intensity profiles were calculated across the whole image, using the ImageJ program (<http://imagej.nih.gov/ij/>). For each profile the width at half-maximum (WHM) was calculated.

Preliminary 3D reconstructions of [Lys3]gA clusters were calculated using angular reconstitution<sup>45</sup> with imposing C4, C5 and C6 symmetry. The C5 symmetry gave the smallest error during reconstruction, thus this type of symmetry was imposed on the final structure. The structure of [Lys3]gA cluster was determined at 2.8-nm resolution. Fitting five right-handed double stranded antiparallel helical dimers (PDB ID: 2IZQ)<sup>46</sup> into the obtained electron density revealed good agreement with the size of the cluster.

## 2.6 Molecular modeling of [Lys3]gA oligomers

As gA contains tryptophans at positions 9, 11, 13, 15, a few discrete modes of dimer-dimer interfaces involving tryptophans can be proposed. Modeling of [Lys3]gA oligomers was based on the crystal structure of gA in complexes with monovalent cations (PDB ID: 1AV2)<sup>47</sup> that represents dimer of right-handed antiparallel  $\beta\beta^{7,2}$  DHs<sup>47</sup> stabilized by stacking of W11 indole rings from neighboring DHs. These “W11-W11” dimers of DHs cannot form larger structures, including those enclosed into a barrel-stave pore. However, the rotation of one partner in this DH dimer by 2 residues ( $\sim 100^\circ$ ) along the double-helix axis resulted in formation of an alternative DH dimer with stacked indole rings of W9 and W11 at the dimerization interface. These “W9-W11” DH dimers can be easily encircled by rotational and translational transformations into a pentagon structure with the interior angles of  $108^\circ$  (Fig. 8). The obtained model of 5-mer was minimized (200 steps) with CHARMM force field implemented in QUANTA (Accelrys Inc.) using a dielectric constant ( $\epsilon$ ) of 10 and the adopted-basis Newton-Raphson method. The coordinate file of the pentamer model can be obtained upon request.

## 3. Results

### 3.1 N-terminal Lys- and Arg- substituted gA analogues induce CF leakage from liposomes

According to our previous study,<sup>28</sup> [Lys3]gA and [Lys1]gA, but not [Glu3]gA, [Glu1]gA and unaltered gA, induced leakage of fluorescent markers from liposomes via formation of large-diameter pores. Here we extended the series of gA analogues and examined those having arginine or histidine at the N terminus. For these experiments, liposomes were loaded with the fluorescent dye CF at a high concentration (100 mM), so that the fluorescence was initially strongly reduced due to concentration quenching. As can be seen from Fig.1,

[Arg3]gA and [Arg1]gA induced the leakage of CF from liposomes, similar to [Lys3]gA, whereas [His1]gA and [His3]gA did not induce the CF leakage at pH 7.0. Anionic peptides ([Glu1]gA, [Glu3]gA, [Asp1]gA) and unaltered gA were also inactive in this system (data not shown). To assess the level of complete release of entrapped CF from liposomes, the detergent Triton X-100 was added at the end of each experiment (100 % level of leakage) and used to normalize the fluorescence response.

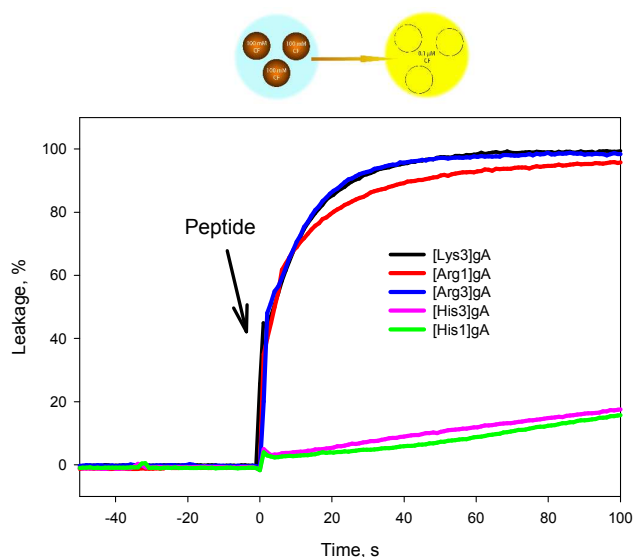


**Fig.1.** The CF leakage from liposomes induced by Lys-, Arg- and His-substituted gA analogues. gA analogues (1  $\mu\text{M}$ ) were added to CF-loaded liposomes (EggPC, 2  $\mu\text{g}/\text{ml}$ ) in Tris/MES buffer, pH=7.0. The cartoon illustrates the increase of CF fluorescence intensity due to reduced concentration quenching of CF fluorescence upon CF release from liposomes.

### 3.2 [Lys3]gA-induced pores allow permeation of molecules with diameter about 1.6 nm

To estimate the pore size, we probed the liposomal leakage of SRB and rhodamine-labeled dextrans with molecular masses of 3 kDa and 10 kDa. In these experiments we used FCS, enabling to monitor the fluorophore release under the conditions of its low (non-quenching) concentration in liposomes. As shown in our previous paper,<sup>48</sup> the amplitude of the autocorrelation function measured under stirring conditions is a sensitive parameter reflecting the leakage of a fluorescent marker from liposomes. The amplitude of the autocorrelation function is inversely proportional to the number of fluorescent particles ( $N=1/G(\tau \rightarrow 0)$ ), where particles can be any fluorescent “point objects” in comparison to the dimension of the observation volume (i.e. about  $1 \mu\text{m}^3$ ). Initially (before the leakage induction) the system has a limited number of particles per observation volume comprising predominantly several dye-

loaded liposomes. After the leakage, the number of particles increases tremendously, because every liposomal particle produces thousands of particles of free dye leading to a significant decrease in the parameter  $G(\tau \rightarrow 0)$ . Fig.2 displays autocorrelation functions of fluorescence of markers entrapped and released from liposomes before and after 5-min incubation with [Lys3]gA (red curves), and also after the addition of Triton X-100 (grey curves), leading to rapid complete efflux of a fluorescent marker. From comparison of panels A, B and C it is seen that [Lys3]gA caused complete leakage of SRB (Fig.2A), but insignificant leakage of 3-kDa dextran (Fig.2B), and no leakage of 10-kDa dextran from liposomes (Fig.2C). Even a slight increase, but not a decrease, of the autocorrelation function can be noticed in Fig.2C. Thus the diameter of [Lys3]gA-induced pores should be smaller than the hydrodynamic diameter of 3-kDa dextran reported to be  $2.33 \pm 0.38$  nm,<sup>49</sup> but larger than the diameter of rhodamine B estimated as 1.6 nm.<sup>50</sup> Of note, the diameter of fluorescein was found to be 0.7 nm.<sup>51</sup>

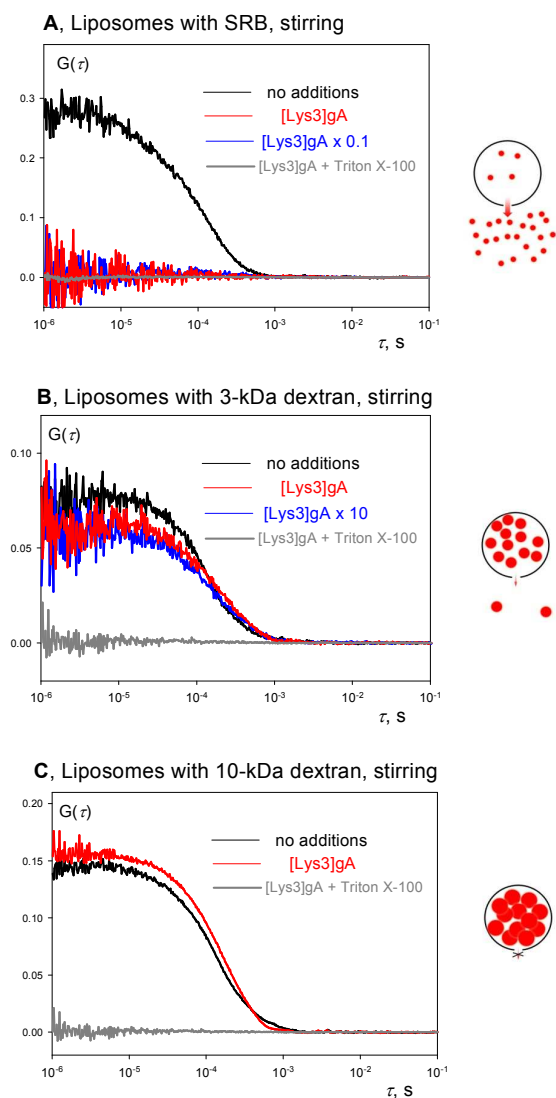


**Fig.2.** Effect of [Lys3]gA on the leakage from liposomes of fluorescent markers: sulforhodamine B (panel A), 3-kDa dextran (panel B), and 10-kDa dextran (panel C). Dye leakage was monitored using FCS. Autocorrelation functions of the marker-loaded liposomes were measured after 5-min incubation with 1  $\mu$ M [Lys3]gA (red curves), without [Lys3]gA (control; black curves), after the addition of 0.1 % Triton X-100 (grey curves). Liposomes were prepared from soybean PC with cardiolipin (80:20 by weight) in Tris/MES buffer, pH 7.4. Lipid concentrations were 0.2  $\mu$ g/ml (panel A), 2  $\mu$ g/ml (panel B), and 2  $\mu$ g/ml (panel C). Blue curve in panel A was recorded with 0.1  $\mu$ M [Lys3]gA, blue curve in panel B was recorded with 10  $\mu$ M [Lys3]gA.

### 3.3 gA inhibits formation of [Lys3]gA-induced pores

In further experiments we studied the effect of unaltered gA on the CF leakage from liposomes. Simultaneous addition of gA and [Lys3]gA induced the CF leakage with smaller rate and amplitude than the leakage caused by [Lys3]gA alone (compare black and green curves in Fig.3). The 5-min preincubation of liposomes with gA before addition of [Lys3]gA

induced leakage that was even more suppressed (grey curve). Thus, gA not only was unable to induce the CF leakage from liposome (red curve in Fig.3), but also suppressed the CF leakage induced by [Lys3]gA. The addition of gA in the course of [Lys3]gA-mediated CF leakage led to deceleration of the CF release in the time scale of minutes resulting in complete retention of a part of the dye (data not shown) suggesting that the process of [Lys3]gA clustering was reversible. Interestingly, although the Trp-free cationic peptide [Lys3Ile9Ile11Ile13Ile15]gA also did not induce the leakage of CF from liposomes (blue curve in Fig.3), it was much poorer inhibitor of the [Lys3]gA-mediated CF leakage than gA (pink and cyan curves in Fig.3).

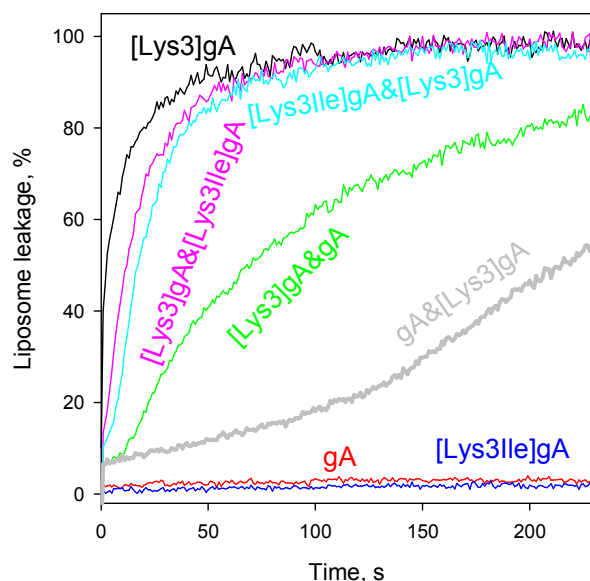


**Fig.3.** Inhibition of [Lys3]gA-induced CF leakage from liposomes by gA and its Trp-free cationic analogue, [Lys3Ile9Ile11Ile13Ile15]gA. [Lys3]gA was added at  $t=0$  min; gA was added at  $t=0$  min (green curve) or 5 min prior to the addition of [Lys3]gA (grey curve); [Lys3Ile9Ile11Ile13Ile15]gA (denoted as [Lys3Ile]gA) was added at  $t=0$  min (pink curve) or 5 min prior to the addition of [Lys3]gA (cyan curve). Red and blue curves correspond to negative controls without [Lys3]gA. Concentrations were: EggPC, 2  $\mu\text{g}/\text{ml}$ ; peptides, 0.1  $\mu\text{M}$ . The buffer contained 100 mM KCl, 10 mM Tris, 10 mM MES, pH 7.

Fig.4A presents a series of CF leakage curves induced by [Lys3]gA after 2-min incubation with different concentrations of gA. At a gA/[Lys3]gA ratio of 0.2:1 (red curve) half inhibition of the leakage was obtained, while at the 1:1 ratio of the peptides the CF leakage was fully suppressed (green curve). Fig.4B shows the dependence of the leakage on

the gA/[Lys3]gA ratio in a broad concentration range.

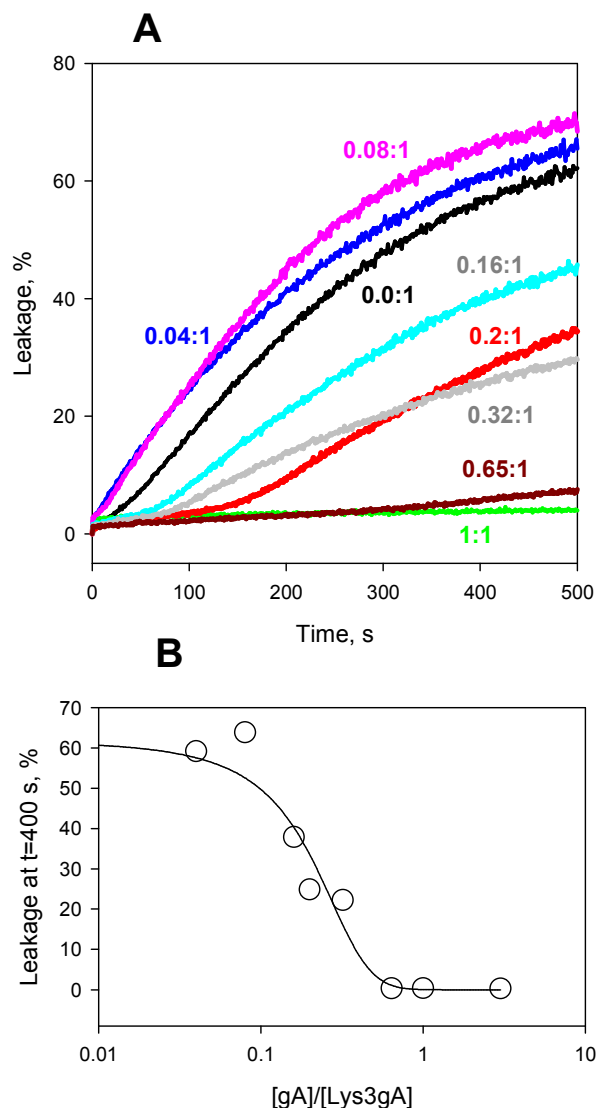


**Fig.4.** Dependence of [Lys3]gA-induced CF leakage from liposomes on concentration of gA. gA was added to liposomes 2 min prior to the addition of [Lys3]gA. Concentrations were: lipid, 2  $\mu\text{g}/\text{ml}$ ; [Lys3]gA, 0.1  $\mu\text{M}$ . Liposomes were prepared from total lipid of *E. coli* in Tris/MES buffer pH 7.

It is known that the charge of lysine depends on pH, and the peptide becomes neutral at pH 11. If the formation of unselective pores actually requires the presence of the cationic charge on the Lys-substituted gA analogue, then alkalization of the medium to pH 11 would substantially inhibit the pore-forming activity of the peptide. We tested this prediction in leakage experiments with SRB, because SRB fluorescence is independent of pH,<sup>52</sup> unlike CF fluorescence which is dramatically pH-dependent.<sup>53</sup> Fig.5A shows concentration dependences of the [Lys3]gA-induced SRB leakage at pH 7 and pH 11, as measured by a decrease in the amplitude of the autocorrelation function using the following equation:<sup>48</sup>

$$\alpha(t) = 1 - \sqrt{\frac{G^t(\tau \rightarrow 0)}{G^0(\tau \rightarrow 0)}} \quad (1)$$

where  $\alpha(t)$  is the portion of the released SRB,  $G^0(\tau \rightarrow 0)$  and  $G^t(\tau \rightarrow 0)$  represent amplitudes of autocorrelation functions  $G(\tau)$  in the limit  $\tau \rightarrow 0$  at the moment of the peptide addition (zero time) and  $t$  min after the addition, respectively. It is seen from Fig.5A that at intermediate peptide concentrations (about 0.1  $\mu\text{M}$ ) there was a pronounced difference in the membrane-permeabilizing potencies of [Lys3]gA at pH 7 and at pH 11: the peptide induced practically complete leakage of SRB at pH 7 after 5-min incubation, whereas modest leakage of the dye was observed at pH 11. These data support the requirement of the cationic charge of lysine for pore formation by [Lys3]gA yielding the dye leakage.

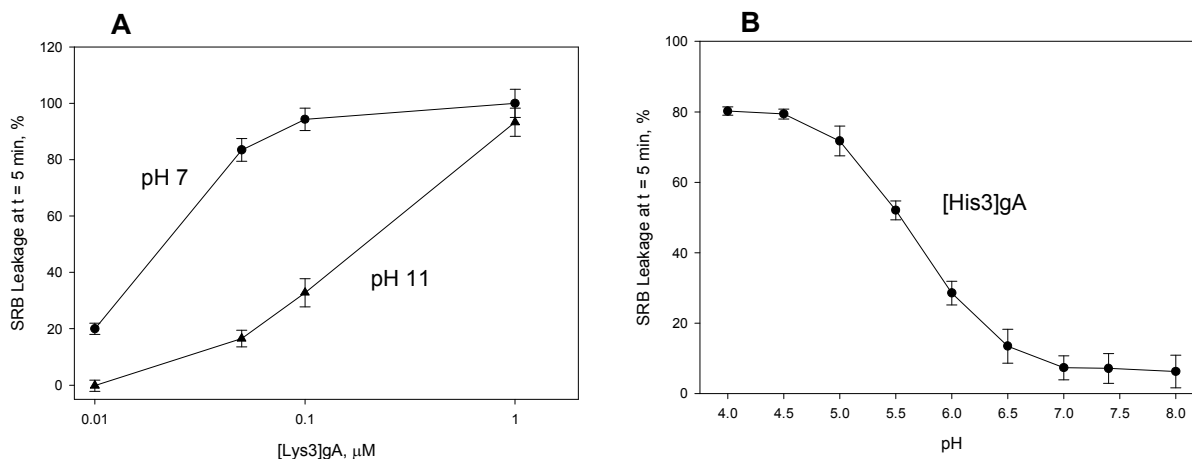


**Fig.5. A.** Dependence of [Lys3]gA-induced leakage of sulforhodamine B from liposomes on the concentration of [Lys3]gA at pH 7 (circles) and pH 11 (triangles) measured by FCS. **B.** pH dependence of the [His3]gA-induced leakage of sulforhodamine B from liposomes. The leakage was estimated from the ratio of the autocorrelation functions of the SRB-loaded liposomes after 5-min incubation with [Lys3]gA (or [His3]gA) and before the addition of the peptide using equation (1). Concentrations were: lipid, 2  $\mu\text{g}/\text{ml}$ ; [His3]gA, 10 nM. Liposomes were made from soybean phosphatidylcholine with cardiolipin (80:20 by weight). The buffer was 100 mM KCl, 10 mM Tris, 10 mM MES, 10 mM  $\beta$ -Alanine.

As shown above, histidine-substituted gA peptides did not induce leakage from liposomes (Fig.1), which could be attributed to a low degree of histidine protonation at pH 7.0 due to its pKa of about 6.5. In fact, lowering pH led to activation of SRB leakage induced by

[His3]gA (Fig.5B). This result highlights the requirement of the cationic charge for the formation of large pores leading to leakage of liposomes.

### 3.4 TEM images indicate formation of oligomeric [Lys3]gA-induced pores

TEM studies were conducted to examine the structure of pores formed by gA analogues in liposomes. Fig.6 shows the examples of TEM images of control liposomes (a), liposomes with unaltered gA (b), liposomes with [Lys3]gA (c) and liposomes with the mixture of [Lys3]gA and gA (d). The membrane of liposomes containing [Lys3]gA was almost 20% thinner, than that of the control EggPC liposomes, and 10% thinner, than that of the liposomes containing unaltered gA (Fig.6e). The gA-caused thinning of the lipid bilayer is in agreement with earlier X-ray diffraction data on modulation of bilayer thickness by gA,<sup>54</sup> which was associated with hydrophobic mismatch between the gA channel length and the membrane thickness.

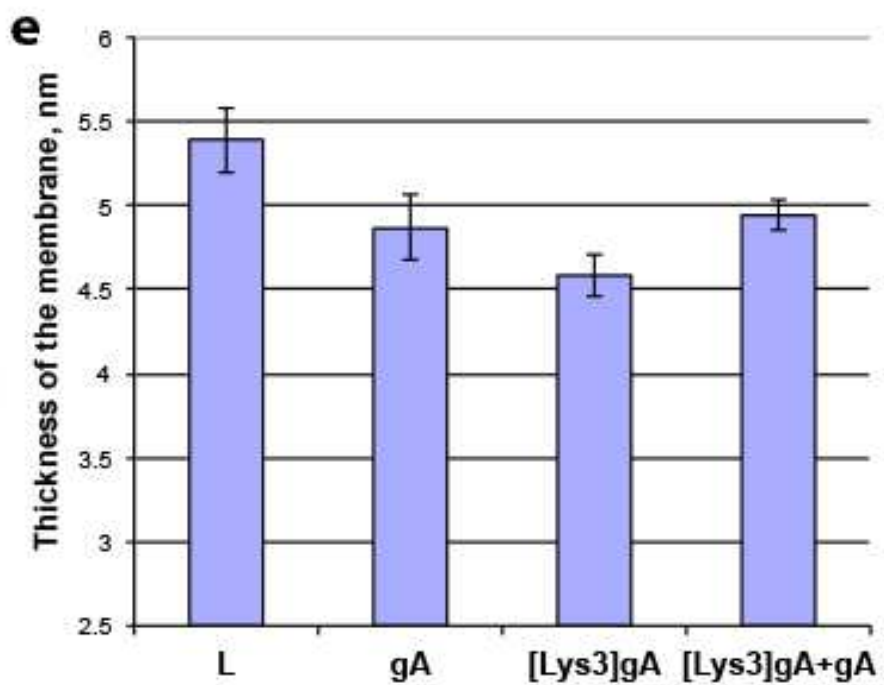
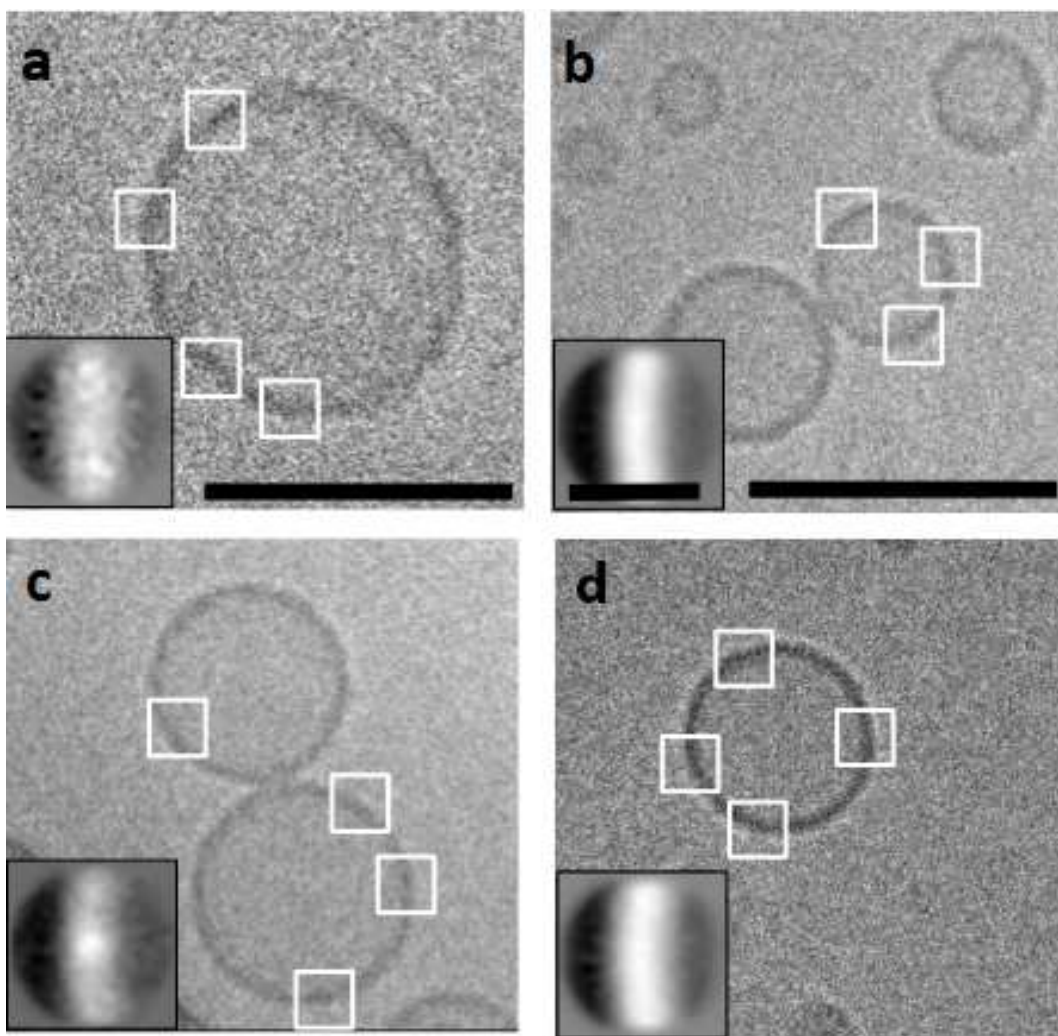


**Fig.6.** TEM images of intact liposomes formed from EggPC (a); gA-containing liposomes (b); [Lys3]gA-containing liposomes (c); liposomes containing both gA and [Lys3]gA (d). Bar – 100 nm. White rectangles show the parts of the liposome membrane selected for further analysis. Inserts – class-sum averages of selected and subsequently aligned liposome membrane parts. Bar – 10 nm. (e) Values of the lipid bilayer thickness for all studied liposomes (L, liposomes without peptides; gA, liposomes with gA; [Lys3]gA, liposomes with [Lys3]gA; [Lys3]gA+gA, liposomes with a mixture of gA and [Lys3]gA).

To compare liposomes with and without gA, we cut the pieces from the liposome images, combined, aligned and superimposed them to obtain the projection images of the lipid bilayers (panels a-d in Fig.7). This procedure greatly increased the signal-to-noise ratio for the selected images. The parts of the bilayer images were selected and analyzed in ImageJ program (Fig.7). We calculated the intensity profile within the selected area by summarizing all pixels along the vertical side of the rectangle. The resulting graphical presentation demonstrates that the [Lys3]gA-containing liposomes possess clusters of high intensity. To further increase the signal-to-noise ratio and better visualize the clusters, we subtracted the structure of a control liposome and that of a gA-containing liposome from the structure of a [Lys3]gA-containing liposome (Fig.7). Both difference images revealed clearly visible clusters with the dimensions of the order of 4 nm across, and with the same thickness as the membrane. Thereby we obtained 30 different cluster projection structures (some examples are shown on Fig.7e). Most of the projections represent the side views of the cluster, and we additionally collected and similarly processed the other views of the clusters (including top views). Based on the CD data showing that antiparallel DH is a predominant form of [Lys3]gA at pH 7,<sup>27</sup> we assume that clusters found in the images represent oligomers of DH. Obviously, clusterization may yield various structures including tetramer, pentamer, hexamer of DH, etc.

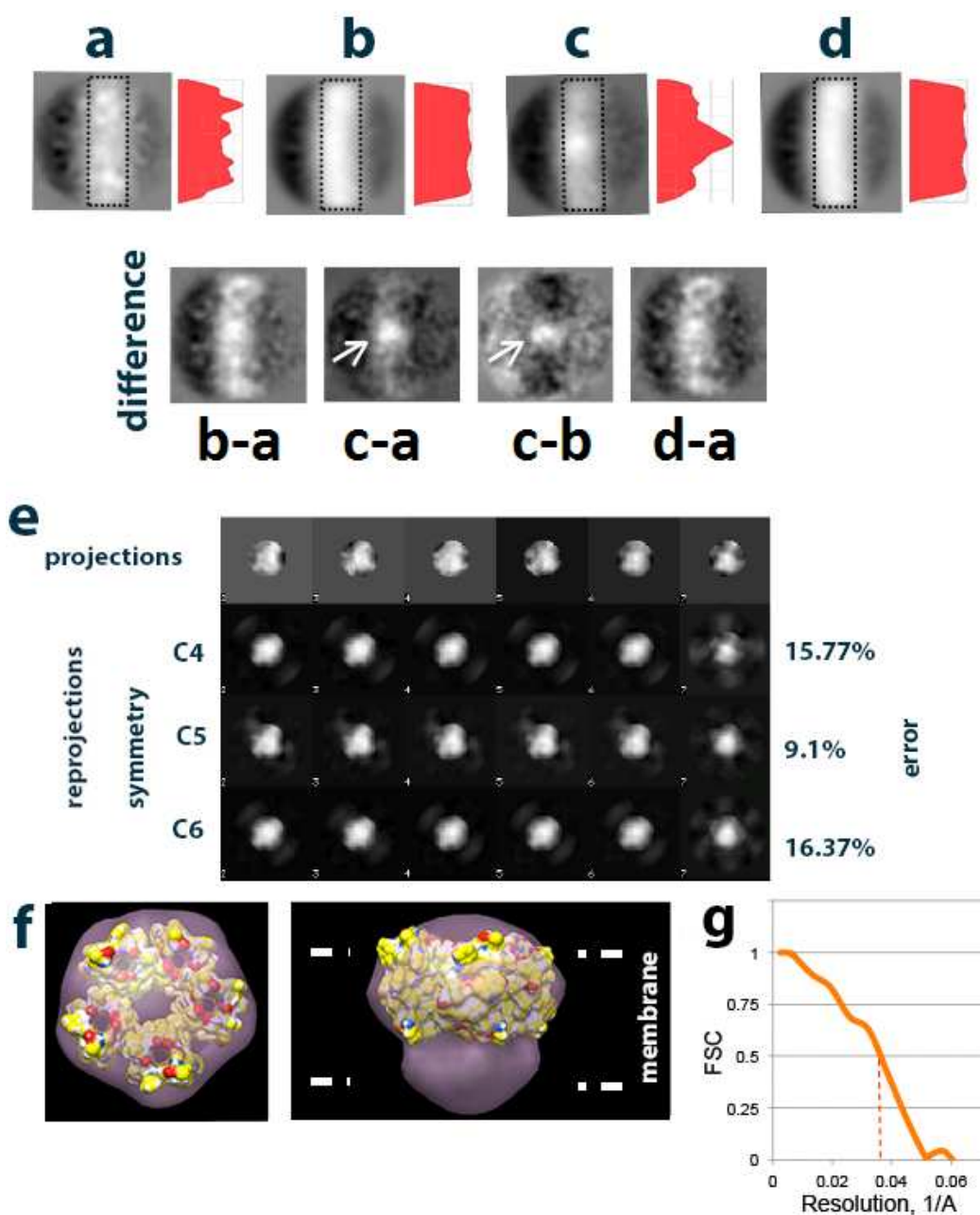


**Fig.7.** TEM study of cluster formation in [Lys3]gA-containing liposomes. (a-d) Projection structures (computed from N images) of (a) intact liposome, N=1534; (b) gA-containing liposome, N=627; (c) [Lys3]gA-containing liposome, N=312; (d) liposome containing both gA and [Lys3]gA, N=450. The membrane is shown with a dotted rectangle. On the right of each projection structure, the intensity profile within this rectangle is shown in red. Bottom row – from left to right: difference maps of the structures in (a) and (b); in (c) and (b); in (c) and (a); in (d) and (b). Arrows are pointing to the cluster in the membrane of a [Lys3]gA-containing liposome; (e) Image processing of [Lys3]gA clusters: row 1 – projections, used for 3D reconstruction; rows 2-4 – re-projections of the 3D reconstruction, using C4, C5 and C6 symmetry, respectively. Corresponding reconstruction error is specified on the right. (f) 3D reconstruction of the [Lys3]A cluster. Left, top view; right, side view. White dotted line marks the borders of the lipid membrane. The pentameric DH model (PDB ID: 2IZQ), represented as a molecular surface, docked into the EM density using UCSF Chimera. (g) Resolution curve calculated according to Fourier Shell Correlation (FSC) between two halves of the data

containing odd and even number of particles. The resolution at the 0.5 correlation level is 2.8 nm.

We used IMAGIC5 and the angular reconstitution method<sup>44</sup> to obtain the 3D structure of the cluster (Fig.7f) using different C-type symmetry at the last reconstruction stage. The pentameric structure was the most realistic one because it had the smallest reconstruction error (Fig.7e) and the DH model obtained by UCSF Chimera<sup>55</sup> demonstrated the most accurate fit into the pentameric 3D reconstruction (Fig.7f). We failed to resolve the pore within our 3D reconstruction, as at the resolution obtained (2.8 nm) it was impossible, consistent with the previous results for potassium channels.<sup>56</sup> It should be pointed out that the conclusion about the pentameric nature of the [Lys3]gA clusters was drawn from the analysis of the ensemble of many clusters. Therefore, better fitting of the pentameric model of the peptide pore could be a result of statistical predominance of this arrangement or the result of domination of the pentameric form over other forms. Further work should answer the question.

### 3.5 Stabilization of [Lys3]gA oligomers through W9-W11 and K3-W13/W15 interactions

The model of a [Lys3]gA oligomer was generated independently of TEM data. Analysis of available crystal structures indicates that gA tends to form large multimeric complexes. For example, dimers stabilized by W11-W11 stacking interactions were found for right-handed  $\downarrow\uparrow\beta\beta$ <sup>7,2</sup> DHs.<sup>46,47</sup> Infinite chains linked by hydrogen bonding between the N-termini were observed for left-handed  $\downarrow\uparrow\beta\beta$ <sup>5,6</sup> DHs.<sup>57</sup> Trimers of left-handed  $\downarrow\uparrow\beta\beta$ <sup>5,6</sup> DHs interacting through tryptophan side chains and co-crystallized lipids formed crystal packing arrangement in lipidic mesophases.<sup>58</sup> The best packing interactions were observed in the dimer of  $\downarrow\uparrow\beta\beta$ <sup>7,2</sup> DHs (PDB IDs: 1AV2, 1BDW, 2IZQ), where indole rings of four W11 from neighboring DHs formed aromatic and van-der-Waals interactions.

The tentative model of a [Lys3]gA oligomer, which was generated using  $\downarrow\uparrow\beta\beta$ <sup>7,2</sup> DHs (as described in Methods), represents a pentamer with a large central pore of  $\sim 10$  Å internal diameter. This pore is large enough to accommodate CF, but requires some side chain movement to allow passage of SRB (Fig.8). Stabilizing intermolecular interactions involve W9-W11 aromatic interactions between contacting DHs. In addition, cation- $\pi$  interactions are present between amino groups of ten K3 and indole rings of W15 or W13 from neighboring DHs. As observed in the model,

each K3 is located between two indole rings (from its-own DH and the neighboring DH) and has geometry that meets distance and angular requirements for cation- $\pi$  interactions.<sup>59</sup>

The modeling of pentameric structure of  $\downarrow\uparrow\beta\beta^{7,2}$  DHs is consistent with our TEM data, including the 3D reconstruction of TEM images and the evaluation of thickness of liposome membranes. In agreement with results of TEM studies indicating that [Lys3]gA induces larger membrane thinning than gA, we found that hydrophobic thickness calculated by the PPM method<sup>60</sup> of modeled 5-mer [Lys3]gA was 20 Å, compared to 23 Å for head-to-head single-stranded  $\beta\beta^{6,3}$  HD (PDB ID: 1GRM) and ~30 Å for the left-handed  $\uparrow\downarrow\beta\beta^{5,6}$  DH (PDB ID: 3ZQ8).

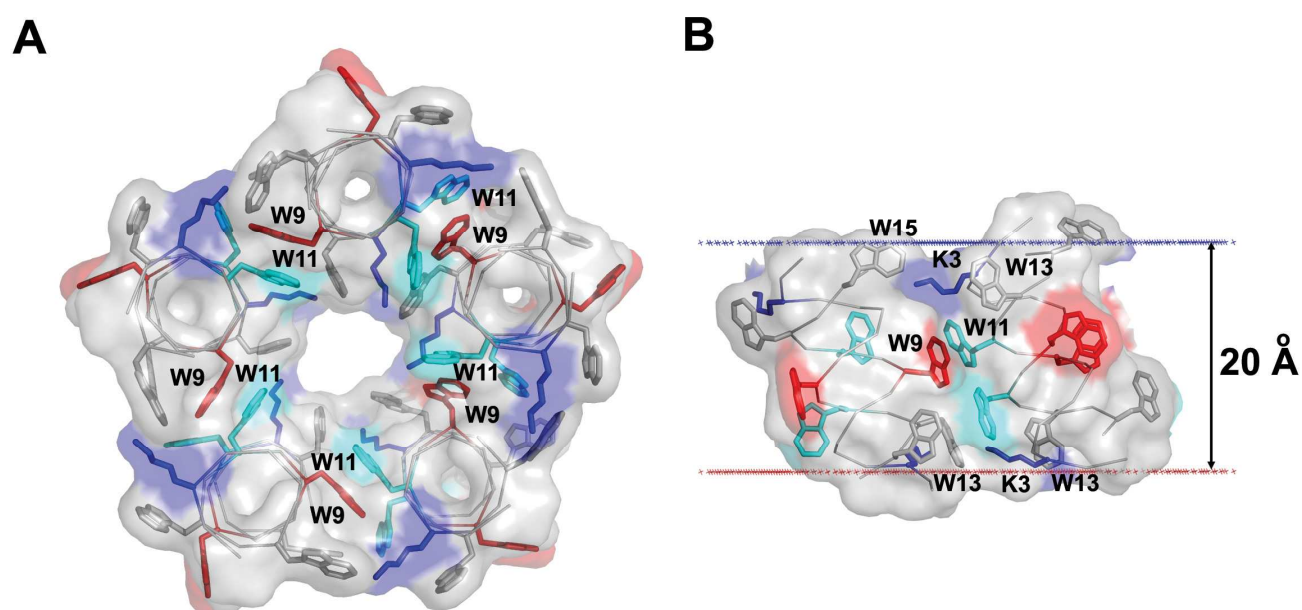


**Fig.8.** Tentative molecular model of 5-mer of [Lys3]gA; top view (A): side view of two neighboring DHs from the 5-mer (B). Pentamer of right-handed  $\downarrow\uparrow\beta\beta^{7,2}$  DHs is shown in surface representation colored light grey, main chain of double helices is shown by ribbon, tryptophan and lysine residues forming intermolecular contacts are shown by sticks colored blue (K3), red (W9), cyan (W11), grey (W13 and W15). Hydrophobic membrane boundaries (at the level of lipid carbonyl groups) calculated by PPM are shown by horizontal red and blue dotted lines (B). Images were produced using PyMOL (at [www.pymol.org](http://www.pymol.org)).

#### 4. Discussion

We propose that the process of pore formation by [Lys3]gA in lipid membranes involves two distinct stages: formation of the antiparallel double helix (DH) from two monomers followed by clusterization of DH yielding a DH pentamer. According to CD data,<sup>27</sup> antiparallel DH represents the major conformation of [Lys3]gA in membranes of liposomes at neutral pH. The mechanism of clusterization of double helices is unclear. We suppose that this process is driven by both aromatic interaction of tryptophans and cation- $\pi$  interaction between cationic amino acid residues (one or two of them on both sides of the membrane) of one DH and one or several tryptophans of the neighboring DH leading to circular clusters having central aqueous lumen. Cation- $\pi$  interactions, particularly between Lys and Trp, were previously found to significantly enhance the strength of oligomerization of hydrophobic helices in a membrane environment.<sup>61</sup> The involvement of cation- $\pi$  interactions in the formation of protein tertiary structure was discovered earlier by bioinformatics analysis<sup>62</sup> and confirmed by molecular dynamics simulation.<sup>63,64</sup> Cation- $\pi$  interactions were also found to participate in the formation of some enzyme-substrate complexes,<sup>65</sup> as well as in oligomerization of HIV-1 Vpr protein.<sup>66</sup>

The involvement of cation- $\pi$  interactions in the formation and/or stabilization of the pore structure by [Lys3]gA and other cationic gA analogues is favored by the following observations: 1) basic amino acid residues are required for the induction of liposome leakage, which is proved by the fact that [Lys3]gA, [Lys1]gA, [Arg1]gA, and [Arg3]gA are active, while [Glu1]gA, [Glu3]gA, and [Asp1]gA along with unaltered gA are inactive, 2) [Lys3Ile9Ile11Ile13Ile15]gA, having lysine in position 3 similar to [Lys3]gA but lacking tryptophans, is unable to form large pores, 3) the induction of pore formation by [Lys3]gA and [His3]gA depends on pH, being suppressed upon alkalization, 4) unaltered gA inhibits pore formation by [Lys3]gA. The latter result supports our model implying that cation- $\pi$  interactions between tryptophan and charged lysine residues indeed stabilize the circular oligomer of [Lys3]gA. If at least one monomer of [Lys3]gA is replaced by that of gA lacking the charged residue, the circular oligomer would be broken, thereby resulting in the loss of the ability to form the barrel-stave pore in the membrane. In the case of pentameric arrangement of the [Lys3]gA pore, it would be sufficient to add gA at the one fifth ratio to [Lys3]gA to inhibit [Lys3]gA-induced membrane leakage. Fig.4B illustrates such an experiment.

The histidine-substituted gA derivatives [His1]gA and [His3]gA were unable to induce the dye leakage of liposomes at pH 7, although a histidine residue in the cationic form is known to exert cation- $\pi$  interaction with tryptophan in membrane peptides.<sup>66</sup> The inactivity of

[His1]gA and [His3]gA in pore formation could be due to the fact that the majority of histidine residues are uncharged at neutral pH (pKa of histidine is about 6.5), rendering cation- $\pi$  interaction unstable. Actually in the M2 protein from the influenza A virus, the cation- $\pi$  interaction between His37 and Trp41 causes opening of a proton channel only at pH below 5.8, whereas at neutral pH the channel is closed.<sup>67</sup> In agreement with this consideration, the decrease in pH of the solution led to stimulation of [His3]gA-mediated dye leakage from liposomes.

As an alternative to cation- $\pi$  interactions, the requirement of amino acid residues with positively charged side chains for the induction of large pores by N-terminally substituted gA derivatives could be ascribed to interaction of the cationic residues with phosphate groups of phospholipids,<sup>68</sup> leading to peptide clusterization and pore formation. However, it is unclear how phosphate groups can provoke peptide oligomerization. Besides, within this mechanism, it is difficult to explain several experimental findings: 1) the inability of the cationic peptide [Lys3Ile9Ile11Ile13Ile15]gA lacking tryptophan residues to induce the liposome leakage (Fig.3), 2) the inhibiting effect of gA on the [Lys3]gA-induced leakage and clusterization of [Lys3]gA, 3) the essential dependence of the pore-forming activity of the Lys-substituted peptides on Lys position in the gA sequence, being maximal for [Lys3]gA among the substitutions in the positions 1, 3, and 5<sup>28</sup> (on the contrary, interaction with phosphate groups is expected to be maximal for the terminal position of Lys in the gA sequence). Therefore, intermolecular cation- $\pi$  interactions between peptide residues are most likely responsible for clusterization of [Lys3]gA and related peptides leading to formation of large pores in lipid membranes.

### Acknowledgements

The authors are grateful to Andrei Lomize from the University of Michigan and Tatyana Rokitskaya from Belozersky Institute of Physico-Chemical Biology for fruitful discussions and a help in conducting several experiments. Synthesis of gA derivatives and liposome leakage studies were financially supported by RFBR grant № 15-04-01755 to Yuri Antonenko. Cryo-electron microscopy experiments were performed at the User Facilities Center “Structural Diagnostics of Materials” at the A.V.Shoubnikov Institute of Crystallography RAS in Moscow under financial support from RSF (№14-14-00234) to Olga Sokolova. Financial support for modeling part of the research (for Irina Pogozheva) was from the Division of Biological Infrastructure of the National Science Foundation under award number 1145367.

## References

- 1 R. J. Dubos, *J. Exp. Med.*, 1939, **70**, 1-10.
- 2 W. E. Herrell and D. Heilman, *J. Clin. Invest*, 1941, **20**, 583-591.
- 3 D. K. Rao, H. Liu, S. V. Ambudkar and M. Mayer, *J. Biol. Chem.*, 2014, **289**, 31397-31410.
- 4 L. M. Hughes, R. Griffith and R. J. Aitken, *Curr. Med. Chem.*, 2007, **14**, 775-786.
- 5 S. B. Hladky and D. A. Haydon, *Curr. Topics in Membr. Transport*, 1984, **21**, 327-372.
- 6 O. S. Andersen and R. E. Koeppe, *Physiol. Rev.*, 1992, **72**, S89-158.
- 7 D. D. Busath, *Annu. Rev. Physiol.*, 1993, **55**, 473-501.
- 8 E. Bamberg, H. J. Apell, H. Alpes, E. Gross, J. L. Morell, J. F. Harbaugh, Janko, K and P. Lauger, *Federation Proceedings*, 1978, **37**, 2633-2638.
- 9 H. J. Apell, E. Bamberg and H. Alpes, *J. Membr. Biol.*, 1979, **50**, 271-285.
- 10 J. S. Morrow, W. R. Veatch and L. Stryer, *J. Mol. Biol.*, 1979, **132**, 733-738.
- 11 E. W. Russell, L. B. Weiss, F. I. Navetta, R. E. Koeppe and O. S. Andersen, *Biophys. J.*, 1986, **49**, 673-686.
- 12 R. E. Koeppe, J. L. Mazet and O. S. Andersen, *Biochemistry*, 1990, **29**, 512-520.
- 13 G. L. Mattice, R. E. Koeppe, L. L. Providence and O. S. Andersen, *Biochemistry*, 1995, **34**, 6827-6837.
- 14 A. E. Daily, J. H. Kim, D. V. Greathouse, O. S. Andersen and R. E. Koeppe, *Biochemistry*, 2010, **49**, 6856-6865.
- 15 D. W. Urry, *Proc. Natl. Acad. Sci. USA*, 1971, **68**, 672-676.
- 16 E. Bamberg, H. J. Apell and H. Alpes, *Proc. Natl. Acad. Sci. USA*, 1977, **74**, 2402-2406.
- 17 A. S. Arseniev, I. L. Barsukov, V. F. Bystrov, A. L. Lomize and Yu.A. Ovchinnikov, *FEBS Lett.*, 1985, **186**, 168-174.
- 18 R. Smith, D. E. Thomas, F. Separovic, A. R. Atkins and B. A. Cornell, *Biophys. J.*, 1989, **56**, 307-314.
- 19 R. R. Ketchem, W. Hu and T. A. Cross, *Science*, 1993, **261**, 1457-1460.
- 20 F. Separovic, J. Gehrman, T. Milne, B. A. Cornell, S. Y. Lin and R. Smith, *Biophys. J.*, 1994, **67**, 1495-1500 .

- 21 F. Wang, L. Qin, C. J. Pace, P. Wong, R. Malonis and J. Gao, *Chembiochem.*, 2012, **13**, 51-55.
- 22 F. Wang, L. Qin, P. Wong and J. Gao, *Biopolymers*, 2013, **100**, 656-661.
- 23 J. Mao, T. Kuranaga, H. Hamamoto, K. Sekimizu and M. Inoue, *ChemMedChem.*, 2015, **10**, 540-545.
- 24 D. N. Silachev, L. S. Khailova, V. A. Babenko, M. V. Gulyaev, S. I. Kovalchuk, L. D. Zorova, E. Y. Plotnikov, Y. N. Antonenko and D. B. Zorov, *Biochim. Biophys. Acta*, 2014, **1840**, 3434-3442.
- 25 J. M. David, T. A. Owens, S. P. Barwe and A. K. Rajasekaran, *Mol. Cancer Ther.*, 2013, **12**, 2296-2307.
- 26 D. Wijesinghe, M. C. Arachchige, A. Lu, Y. K. Reshetnyak and O. A. Andreev, *Sci. Rep.*, 2013, **3**, 3560.
- 27 T. I. Rokitskaya, A. I. Sorochkina, S. I. Kovalchuk, N. S. Egorova, E. A. Kotova, S. V. Sychev and Y. N. Antonenko, *Eur. Biophys. J.*, 2012, **41**, 129-138.
- 28 A. I. Sorochkina, S. I. Kovalchuk, E. O. Omarova, A. A. Sobko, E. A. Kotova and Y. N. Antonenko, *Biochim. Biophys. Acta*, 2013, **1828**, 2428-2435.
- 29 Y. N. Antonenko, T. B. Stoilova, S. I. Kovalchuk, N. S. Egorova, A. A. Pashkovskaya, A. A. Sobko, E. A. Kotova, S. V. Sychev and A. Y. Surovoy, *FEBS Lett.*, 2005, **579**, 5247-5252.
- 30 T. B. Stoilova, E. A. Dutseva, A. A. Pashkovskaya, S. V. Sychev, S. I. Kovalchuk, A. A. Sobko, N. S. Egorova, E. A. Kotova, Y. N. Antonenko, A. Y. Surovoy and V. T. Ivanov, *Russ. J. Bioorg. Chem.*, 2007, **33**, 474-481.
- 31 W. R. Veatch, E. T. Fossel and E. R. Blout, *Biochemistry*, 1974, **13**, 5249-5256.
- 32 B. A. Wallace, *Annu. Rev. Biophys. Biophys. Chem*, 1990, **19**, 127-157.
- 33 S. V. Sychev, L. I. Barsukov and V. T. Ivanov, *Eur Biophys J*, 1993, **22**, 279-288.
- 34 O. V. Kolomytkin, A. O. Golubok, D. N. Davydov, V. A. Timofeev, S. A. Vinogradova and S. Y. Tipisev, *Biophys. J.*, 1991, **59**, 889-893.
- 35 A. V. Krylov, E. A. Kotova, A. A. Yaroslavov and Y. N. Antonenko, *Biochim. Biophys. Acta*, 2000, **1509**, 373-384.
- 36 Y. N. Antonenko, V. Borisenko, N. S. Melik-Nubarov, E. A. Kotova and G. A. Woolley, *Biophys. J.*, 2002, **82**, 1308-1318.
- 37 A. I. Sorochkina, E. Y. Plotnikov, T. I. Rokitskaya, S. I. Kovalchuk, E. A. Kotova, S. V. Sychev, D. B. Zorov and Y. N. Antonenko, *PLoS One.*, 2012, **7**, e41919.
- 38 I. V. Perevoshchikova, D. B. Zorov and Y. N. Antonenko, *Biochim. Biophys. Acta*, 2008, **1778**, 2182-2190.

- 39 A. Pashkovskaya, E. Kotova, Y. Zorlu, F. Dumoulin, V. Ahsen, I. Agapov and Y. Antonenko, *Langmuir*, 2010, **26**, 5726-5733.
- 40 S. S. Denisov, E. A. Kotova, E. Y. Plotnikov, A. A. Tikhonov, D. B. Zorov, G. A. Korshunova and Y. N. Antonenko, *Chem. Commun.*, 2014, **50**, 15366-15369.
- 41 S. T. Hess, S. Huang, A. A. Heikal and W. W. Webb, *Biochemistry*, 2002, **41**, 697-705.
- 42 O. Krichevsky and G. Bonnet, *Rep. Prog. Phys.*, 2002, **65**, 251-297.
- 43 S. J. Ludtke, P. R. Baldwin and W. Chiu, *J. Struct. Biol.*, 1999, **128**, 82-97.
- 44 M. van Heel, G. Harauz, E. V. Orlova, R. Schmidt and M. Schatz, *J. Struct. Biol.*, 1996, **116**, 17-24.
- 45 M. van Heel, *Ultramicroscopy*, 1987, **21**, 111-123.
- 46 A. Olczak, M. L. Glowka, M. Szczesio, J. Bojarska, W. L. Duax, B. M. Burkhart and Z. Wawrzak, *Acta Crystallogr. D. Biol. Crystallogr.*, 2007, **63**, 319-327.
- 47 B. M. Burkhart, N. Li, D. A. Langs, W. A. Pangborn and W. L. Duax, *Proc. Natl. Acad. Sci. U. S. A.*, 1998, **95**, 12950-12955.
- 48 A. M. Firsov, E. A. Kotova, E. A. Korepanova, A. N. Osipov and Y. N. Antonenko, *Biochim. Biophys. Acta*, 2015, **1848**, 767-774.
- 49 J. J. Choi, S. Wang, Y. S. Tung, B. Morrison, and E. E. Konofagou, *Ultrasound Med. Biol.*, 2010, **36**, 58-67.
- 50 F. Tsunomori and H. Ushiki, *Physics Letters A*, 1999, **258**, 171-176.
- 51 A. Cvetkovic, C. Piciooreanu, A. J. Straathof, R. Krishna and L. A. van der Wielen, *J. Am. Chem. Soc.*, 2005, **127**, 875-879.
- 52 R. W. Chambers, T. Kajiwara, and D. R. Kearns, *J. Phys. Chem.* 1974, **78**, 380-387.
- 53 J. Bramhall, J. Hofmann, R. DeGuzman, S. Montestruque and R. Schell, *Biochemistry*, 1987, **26**, 6330-6340.
- 54 T. A. Harroun, W. T. Heller, T. M. Weiss, L. Yang and H. W. Huang, *Biophys. J.*, 1999, **76**, 937-945.
- 55 T. D. Goddard, C. C. Huang and T. E. Ferrin, *J. Struct. Biol.*, 2007, **157**, 281-287.
- 56 A. Grizel, A. Popinako, M. A. Kasimova, L. Stevens, M. Karlova, M. M. Moisenovich and O. S. Sokolova, *J. Neuroimmune Pharmacol.*, 2014, **9**, 727-739.
- 57 B. M. Burkhart, R. M. Gassman, D. A. Langs, W. A. Pangborn and W. L. Duax, *Biophys. J.*, 1998, **75**, 2135-2146.

- 58 N. Hofer, D. Aragao and M. Caffrey, *Biophys. J.*, 2010, **99**, L23-L25.
- 59 F. N. Petersen, M. O. Jensen and C. H. Nielsen, *Biophys. J.*, 2005, **89**, 3985-3996.
- 60 M. A. Lomize, I. D. Pogozheva, H. Joo, H. I. Mosberg and A. L. Lomize, *Nucleic Acids Res.*, 2012, **40**, D370-D376.
- 61 R. M. Johnson, K. Hecht and C. M. Deber, *Biochemistry*, 2007, **46**, 9208-9214.
- 62 J. P. Gallivan and D. A. Dougherty, *Proc. Natl. Acad. Sci. U. S. A.*, 1999, **96**, 9459-9464.
- 63 E. V. Pletneva, A. T. Laederach, D. B. Fulton and N. M. Kostic, *J. Am. Chem. Soc.*, 2001, **123**, 6232-6245.
- 64 M. P. Aliste, J. L. MacCallum and D. P. Tieleman, *Biochemistry*, 2003, **42**, 8976-8987.
- 65 N. Zacharias and D. A. Dougherty, *Trends Pharmacol. Sci.*, 2002, **23**, 281-287.
- 66 T. Kamiyama, T. Miura and H. Takeuchi, *Biophys. Chem.*, 2013, **173-174**, 8-14.
- 67 H. Takeuchi, A. Okada and T. Miura, *FEBS Lett.*, 2003, **552**, 35-38.
- 68 Y. Su, T. Doherty, A. J. Waring, P. Ruchala and M. Hong, *Biochemistry*, 2009, **48**, 4587-4595.